

https://dspace.org/

# Dynamic Aperture Selection for Turbulence Resilience

**A Vallance; Mark Main; Malik L. Salloum; Mikaeel Dindar; U Daly ...**

IEEE-INST ELECTRICAL ELECTRONICS ENGINEERS INC
https://hdl.handle.net/10539/47369
WOS

Downloaded from a DSpace repository. https://dspace.org/

# Dynamic Aperture Selection for Turbulence Resilience

Adam J. Vallance, Mark Main, Malik L. Salloum, Mikaeel Dindar, Ultan J. Daly, Philip Ginster, Mitchell A. Cox, *Senior Member, IEEE*, and Martin P. J. Lavery

***Abstract*—Free-space optical communication systems are susceptible to atmospheric turbulence causing intermittent deep fading, which results in lost information and channel bit errors. Mitigation techniques typically require complex adaptive optics, digital signal processing or optical amplification to reduce the impact of turbulence. By spacing multiple apertures at distances comparable to the Fried parameter, spatial diversity is introduced, improving turbulence resilience. This paper demonstrates a low complexity implementation of spatial diversity, leveraging four multimode fiber coupled 1Gbps bi-directional Small Form-factor Pluggables, each near collimated by a spatially separated collection for both power combining and channel selective switching at the receiver. Under real-world turbulent conditions a sustained data rate of 1Gbps was achieved with 5.71% of frames dropped with a maximum dropout length of 0.90s over a 24-hour period. Link lengths of up to 1.3km were experimentally demonstrated.**

***Index Terms*—Free-space optical communications, spatial diversity.**

## I. Introduction

UNIVERSAL internet connectivity is a critical enabler for economic development globally. However, many communities are not adequately connected due to economic, geographic and infrastructure security challenges leading to a digital divide [1]. Free-space optical communications (FSOC) offers promise to bridge this digital divide as such links can be quickly and inexpensively installed on rooftops making this economically viable for low-income peri-urban communities. However, for reliable FSOC deployments, it is critical to mitigate environmental factors such as atmospheric turbulence and shifting mechanical alignment. Common approaches include complex adaptive optical systems such as deformable mirrors, MEMS systems, or galvo-mirrors [2], [3]. Non-mechanical mitigation such as Multi-Input-Multi-Output (MIMO) digital signal processing (DSP) or integrated photonic transceivers have been demonstrated, however, each requires complex digital or electro-optical systems [2], [4], [5]. The associated complexity and relative scarcity of the components used in these systems currently prohibit their use in many deployment scenarios.

Spatial diversity improvements were first shown in radio communications to combat multi-path fading [6] and were later extended into MIMO communications [7]. Spatial diversity has since been applied to improve turbulence resilience in optical links [2], [8]. The use of multiple transmitters carrying the same data builds redundancy against channel fading. By spatially separating apertures, atmospheric effects which induce deep fades are isolated to one of several paths. The probability of all channels being in a simultaneous deep fade condition decreases as a function of each added aperture [9]. Despite the potential improvements of spatial diversity for FSOC and the widespread availability of commercial off-the-shelf (COTS) transceivers like the Small Form-Factor Pluggable (SFP) designed for fiber networking, such systems have not yet been widely deployed. Perlot et al. demonstrate an 18km link using SFP+ transceivers however faced challenges in digitally combining multiple receivers in an FPGA [10]. Robust methods to duplicate, combine and switch the outputs from multiple SFP transceivers could allow for the realization of low-complexity deployment of spatial diversity for turbulence mitigation.

In this work, we demonstrate a duplex, spatially diverse FSOC link built using commercial SFP transceivers. Our system which uses a cluster of four 75mm lenses to transmit and receive data through four 1Gbps bi-directional SFPs inserted into a printed circuit board (PCB), is depicted in Fig. 1. Each source will incoherently combine over multiple receiver apertures, providing an increase in power and field of view at the receiver plane. Using an electrical crosspoint switch in real-time, we actively select the routed data channel, avoiding the requirement for complex processing or cross-SFP synchronization. We completed two real-world field trials of our system, over a 1.3km link in Scottish winter coastal conditions and 400m urban deployment in Johannesburg, South Africa, comprising two distinct deployment scenarios for bridging the digital divide.

## II. Methods

### A. Optics

Designing a deployable FSOC link presents significant challenges due to multiple factors which can cause disruption. Atmospheric turbulence causes perturbations in each beam,

Received 24 March 2025; revised 5 June 2025; accepted 22 June 2025. Date of publication 30 June 2025; date of current version 21 October 2025. This work was supported in part by the Engineering and Physical Sciences Research Council, under EPSRC Grant EP/S022821/1, Grant EP/T009012/1, and Grant EP/524359/1; in part by South African National Research Foundation under Grant TTK2204011621; and in part by the Royal Academy of Engineering: Transforming Systems through Partnership—Bytes Over Lights: Levelling Up Community Connectivity With Cost-Effective Optical Wireless Communication under Grant TSP-2324-6\133. *(Adam J. Vallance and Mark Main contributed equally to this work.) (Corresponding author: Martin P. J. Lavery.)*

Adam J. Vallance, Mark Main, Malik L. Salloum, Ultan J. Daly, and Martin P. J. Lavery are with the James Watt School of Engineering, University of Glasgow, G12 8QQ Glasgow, U.K. (e-mail: martin.lavery@glasgow.ac.uk).

Mikaeel Dindar, Philip Ginster, and Mitchell A. Cox are with the School of Electrical and Information Engineering, University of the Witwatersrand, Johannesburg South Africa.

Color versions of one or more figures in this letter are available at https://doi.org/10.1109/LPT.2025.3583079.

Digital Object Identifier 10.1109/LPT.2025.3583079

1041-1135 © 2025 IEEE. All rights reserved, including rights for text and data mining, and training of artificial intelligence and similar technologies. Personal use is permitted, but republication/redistribution requires IEEE permission.
See https://www.ieee.org/publications/rights/index.html for more information.

Authorized licensed use limited to: University of Witwatersrand. Downloaded on October 24,2025 at 06:26:12 UTC from IEEE Xplore. Restrictions apply.

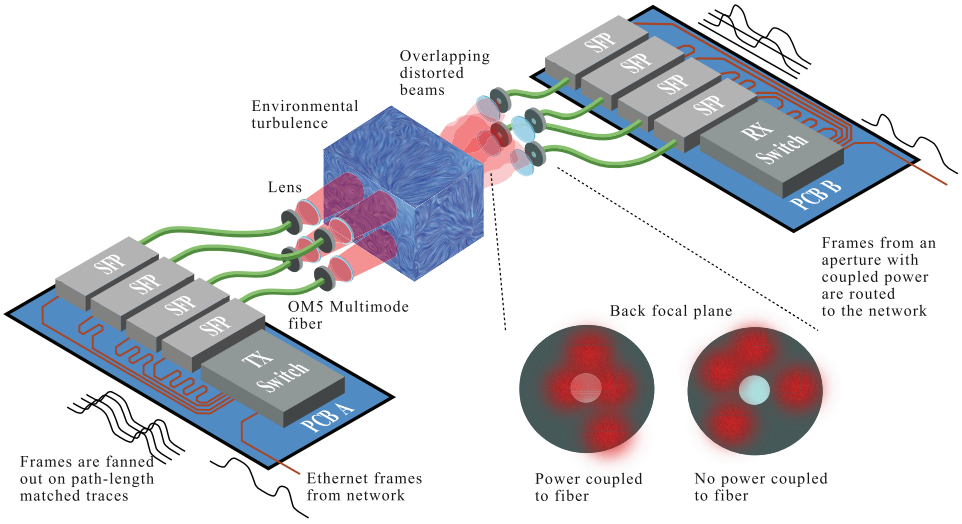


Fig. 1. System diagram of a simplex representation with four apertures at each end of the channel. On the first printed circuit board (PCB), ethernet frames are fanned out onto path-length matched electronic traces which are input to several SFPs. The SFPs are coupled into OM5 Multimode fibres and collimated with a lens. Environmental turbulence causes the propagated beams to be distorted and deflected. The beams are enlarged to appear as large Gaussian spots in the back focal plane. These may overlap to reach the sensitivity threshold. Provided enough power is coupled into one fiber the link will remain functional. The receiver diversity is achieved by electronically routing the SFP signal from an aperture which has coupled optical power.

fluctuating on the order of milliseconds, whilst thermal cycling and direct sunlight may cause simultaneous misalignment of all apertures. To mitigate these challenges, a combination of strategies are integrated to minimize lost frames.

A $2 \times 2$ lens array is established at each end of the bidirectional link. The system is designed with four plano-convex lenses (Edmund Optics 75.0mm Dia. x 150.0mm FL, Uncoated, Plano-Convex Lens). This produces a beam which does not clip at the aperture and matches the numerical aperture of the fiber in the back focal plane to the lens. X-Y translating cage mounts (Thorlabs CXY1A) adjust the fiber position for optimal coupling. We use OM5-graded index multimode fibers. Due to their larger core diameter ($50\mu$m), they have a high numerical aperture and a greater spatial bandwidth, allowing higher-order spatial components introduced by turbulent aberrations to be received, whilst transmitting with near-Gaussian profiles [11]. Each fiber is coupled into a bidirectional SFP. We used 1490nm/1550nm 1Gbps SFP pairs (FS: SFP-GE-BX160). The closely spaced wavelengths facilitate bidirectional alignment.

When attempting to compensate for the atmospheric turbulence, the center-to-center spacing for adjacent lenses was chosen to be 100mm. Given a typical turbulence value of $C_n^2 = 10^{-14}\text{m}^{-2/3}$ for a 400m channel at 1550nm, [12] this gives a Fried parameter of $r_0 = 130$mm, given by $r_0 = \left(0.423\, k^2 C_n^2\, L\right)^{-3/5}$ [13]. This architecture prioritizes feasibility using widely available standard optical components. To ensure fully uncorrelated channels, the apertures would require larger separations, however the fill factor, which is crucial for transmit diversity, could then no longer be maximized using standard lens sizes. While alternative configurations may offer performance gains for specific deployments, our design balances practical implementation constraints to operate in our trials and may be adapted for other scenarios.

Beam defocusing can mitigate turbulence and pointing error at the cost of reducing received power. In a laboratory turbulence chamber, we measured an error-free receiver threshold of −35dBm over a 300s period, operating slightly below the rated SFP sensitivity of −33dBm. We selected −35 dBm as our operating threshold based on this measurement. Trading off ∼25dB of power reduces scintillation whilst leaving sufficient headroom above the threshold to continue operation through some deep fades. Additionally, overlap at the receiver apertures creates transmit diversity where each SFP receives sufficient power from the incoherent addition of the four beams as seen in Fig. 1. Where turbulence interrupts one optical path, the total power at a given aperture can still exceed the threshold. Due to tight receiver sensitivities and minimal ambient coupling into the apertures, provided the SFP receives sufficient power, we do not measure frame losses resulting from ambient light.

### B. Electronics

In the transmit path of each PCB, a crosspoint switch (SN65LVCP408) duplicates the input onto path-length matched (±0.2mm) traces to each SFP. As the beams from multiple SFPs may be summed in the receiving SFP at the other end of the link, the combined beams must be within the minimum 1000Base-BX decision timing offsets for transmitter and dispersion penalty of ±80ps or it may experience performance degradation [14]. The switch has a typical output skew of 25ps, the PCB (FR4 substrate with $\epsilon_r = 4.1$) contributes <2.70ps and the cross-coupled optical path length difference adds 80fs over a 400m link, totaling 27.8ps excluding the SFPs themselves. At 1.25GBd, each bit lasts 800ps so provided total latency offsets are insignificant in comparison, it is unlikely this would cause errors. We tested several sets of SFPs in our PCBs by combining 8 SFP outputs using a fiber beamsplitter and did not observe lost frames or increase in back-to-back bit error rate.

Receiver diversity is created by using a second switch, which routes only one selected aperture's signal for connection

Authorized licensed use limited to: University of Witwatersrand. Downloaded on October 24,2025 at 06:26:12 UTC from IEEE Xplore. Restrictions apply.

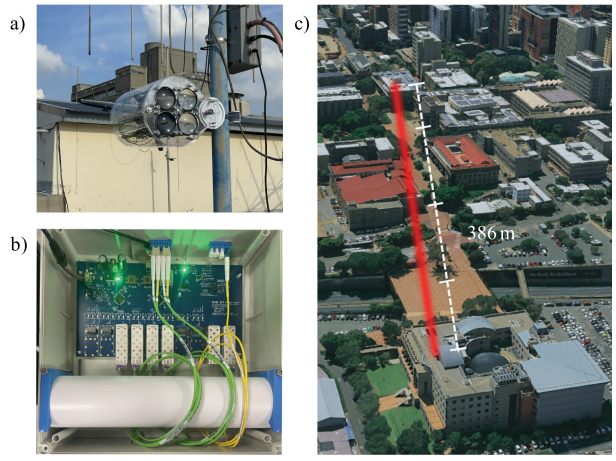


Fig. 2. Experimental setup. a) The Optomechanical setup mounted on a pole. b) Electronics containing SFPs coupled into fibers which lead to apertures. c) An aerial view of the beam path, crossing a highway bridge and campus in Johannesburg. © Vexcel Imaging US, Inc., Google, Airbus, Landsat/Copernicus, Data SIO, NOAA, U.S. Navy, NGA, GEBCO.

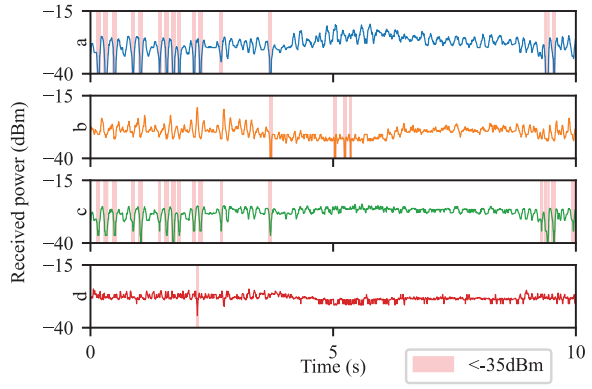


Fig. 3. Instantaneous received powers during a turbulent 10s period. Shaded areas indicate deep fades where the power is below threshold.

**Algorithm 1** Power-Monitoring Channel Selection

**Input:** A list of measured RX powers $P = [p_1, p_2, p_3, p_4]$
**Input:** The low power threshold $P_{\text{threshold}}$
**Input:** The currently selected aperture index $a_{\text{current}}$
  **if** $P[a_{\text{current}}] < P_{\text{threshold}}$ **then**
    $a_{\max} \leftarrow \text{ARGMAX}(P)$
    **route**$(a_{\max})$
    $a_{\text{current}} \leftarrow a_{\max}$
  **end if**

to an external network. The switch time is rated at 15ns which therefore interrupts up to 3 8b/10b symbols. This interruption can cause a maximum of one frame to be discarded as the minimum ethernet payload size is 64 bytes followed by a 12-byte inter-packet gap [14]. If the deep fade lasts longer than one frame, switching will improve uptime. When an ethernet frame is disrupted due to a switch or turbulence, the cyclic redundancy check detects this and discards the corrupted frame. Over Transmission Control Protocol (TCP), a retransmission request will be made for lost frames [15]. We focus on minimizing lost frames with the assumption of limiting usage of our system to TCP/IP over ethernet.

Power readings from four SFPs are measured at an average sample rate of 999Hz. A threshold heuristic must be applied when making switching decisions. When the current aperture has sufficient power, a 'greedy' switch to the instantaneous highest power unnecessarily discards one frame. The instantaneous highest power varies continuously with scintillation in the four channels whereas deep fades we aim to recover from occur sporadically, as seen in Fig. 3. Algorithm 1 focuses on rapid reactions rather than any predictive model.

Running in parallel is an interrupt-driven routine which immediately switches to the next SFP which is receiving power when the loss of signal pin of the currently routed SFP is asserted. This compensated for the maximum frequency of an optical chopper (3163Hz), resulting in a switching rate of 6326Hz implying a response time of $< 158\,\mu s$. These methods are complementary and recover rapidly from deep fades whilst avoiding unnecessary switching.

## III. Results

An initial trial was conducted forming a 1.3km link across a bay in Fairlie, Scotland, during winter, demonstrating an operational range suitable for peri-urban settings. We achieved 1Gbps communications and observed switching rates up to 14.5Hz. Further results refer to the full field trial in South Africa. Weather conditions for both tests are given in Supplemental 1.

The optomechanical mount and PCB, shown in Fig. 2, were installed for both tests. In Johannesburg, we used a modified version of iPerf3, a computer at the eastern (top of c) end of the link would send frames (of 1518 bytes) and a computer on the western end would log dropped frames. Simultaneously, the PC logs PCB output of SFP received powers, along with timestamps and the index of the currently routed aperture.

An illustrative example of 10s of instantaneous powers is presented in Fig. 3. Here we see deep fades occurring on apertures a, b, and c, but not all four simultaneously. We observe correlated deep fades in apertures a and c. Potential causes for this include: mechanical movement of the mounts, updrafts of wind creating miraging effects, or scintillation during momentary periods of increased correlation length. Despite two apertures experiencing simultaneous deep fades, the spatial diversity enables the link to be maintained so long as at least one aperture is above threshold at each moment, as is the case in this sample period.

To assess our methodology's spatial diversity gain, we conducted two consecutive 30-minute tests, near midday, where turbulence was the strongest, for both the $2 \times 2$ array of lenses and a single aperture configuration as shown in Fig. 4. By measuring the duration of loss events, we can quantify the efficacy of our system in switching out of deep fades, reducing the likelihood of noticeable downtime e.g. a 500ms pause may stutter video calls transmitted over the link.

Although the peak lengths of downtime correspond closely for both configurations, the 4↔4 system has a notable reduction in high-loss events, which would cause the greatest issues for end users. Large frame loss events, those $> 10^5$ frames or 1.2 seconds, are minimized by the 4↔4 system as switches are made to recover the link. In this instance, we observed a

Authorized licensed use limited to: University of Witwatersrand. Downloaded on October 24,2025 at 06:26:12 UTC from IEEE Xplore. Restrictions apply.

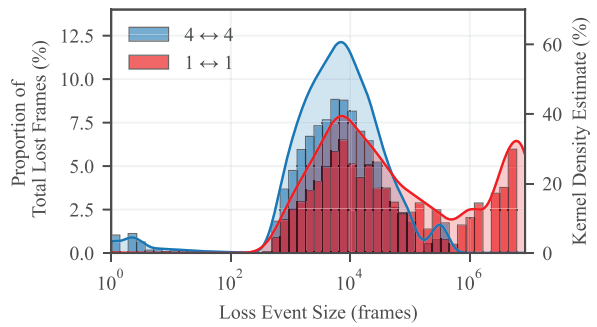


Fig. 4. Comparison of 4↔4 and single channel links run over a half hour period consecutively for the total frame loss over the designated time period based on the event size. Kernel density estimates generate continuous probability distributions for loss event lengths, highlighting the redistribution toward shorter loss events using spatial diversity.

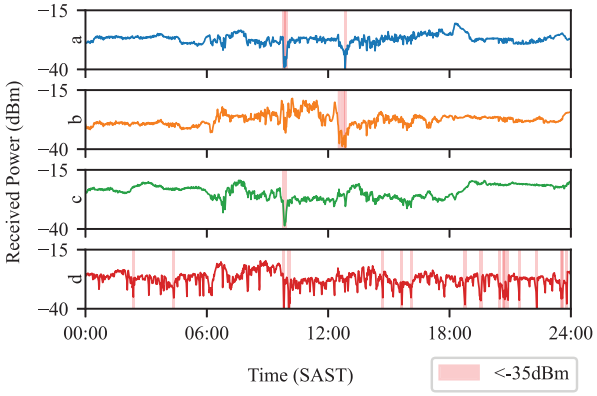


Fig. 5. 24 hours of minute-wise mean powers for each aperture. Times are in South African Standard Time (SAST). Shaded areas indicate that the mean power in that minute period was below the threshold.

60% reduction in total lost frames using the 4↔4 configuration compared to the single channel.

A 24-hour period of minute-wise average receiver powers is shown in Fig. 5. For each minute sample, at least one of the channels is above the threshold of −35dBm indicating that the link was reliable throughout the day. In a), b) and c), during daylight hours more variation is seen with intense sunlight creating strong turbulence whilst the powers show less variation during the night. In d), a 3D-printed tracking system moves the fiber of one aperture in the back focal plane, constantly stepping, see Supplemental 1. Tracking systems are well understood and we include this to demonstrate that such systems can be integrated into our system to overcome temporary misalignments [16]. Over the 24 hours, 4414 switching events occurred with maximum switch rates of 6.13Hz during a one-minute period. In total, 5.71% of frames were lost from switching and fading, with a maximum total dropout length of 0.9s. The low switch rate demonstrates that the combination of the techniques detailed provides resilience to turbulence and was effective at preventing extended dropouts.

## IV. Conclusion

We have presented a spatially diverse free-space optical communications system built from COTS components. Spatial diversity is achieved through an electronic design which allows incoherent combination at the receiver. Using OM5 multimode fiber and defocusing the beams enhances resilience to turbulence and mechanical instability. Whilst the effects of these issues are difficult to uncouple, we have demonstrated a holistic solution which effectively tackles these problems to minimize lost frames. The system successfully transmitted 1Gbps data at a link length of 386m over 24 hours with a maximum drop out time of 0.9s. This demonstrates effective turbulence mitigation without adaptive optics, DSP, or transmit amplification using a combination of techniques. In future work, this method could be extended to 10Gbps by using SFP+ transceivers with a faster crosspoint switch. Fiber alignment of each aperture is the main challenge, which would be assisted by further development of the motorized XY flexure in both hardware and software. This development sets a promising future for the use of COTS components in small-scale deployable FSOC systems, which are ultimately needed in the efforts to tackle the digital divide.

## Acknowledgment

The authors appreciate the support of Graham M. Gibson in carrying out this research.

## References

[1] M. P. J. Lavery et al., "Tackling Africa's digital divide," *Nature Photon.*, vol. 12, no. 5, pp. 249–252, Apr. 2018.
[2] X. Zhu and J. M. Kahn, "Free-space optical communication through atmospheric turbulence channels," *IEEE Trans. Commun.*, vol. 50, no. 8, pp. 1293–1300, Aug. 2002.
[3] A. Trichili, M. A. Cox, B. S. Ooi, and M.-S. Alouini, "Roadmap to free space optics," *J. Opt. Soc. Amer. B, Opt. Phys.*, vol. 37, no. 11, p. 184, Nov. 2020.
[4] A. Billaud et al., "Free space optical link demonstration using multi-plane light conversion turbulence mitigation," *Proc. SPIE*, vol. PC11993, Apr. 2022, Art. no. PC1199302.
[5] V. Billault et al., "Free space optical communication receiver based on a spatial demultiplexer and a photonic integrated coherent combining circuit," *Opt. Exp.*, vol. 29, no. 21, p. 33134, Oct. 2021.
[6] W. M. Sharpless, "Measurement of the angle of arrival of microwaves," *Proc. IRE*, vol. 34, no. 11, pp. 837–845, Nov. 1946.
[7] P. W. Wolniansky, G. J. Foschini, G. D. Golden, and R. A. Valenzuela, "V-BLAST: An architecture for realizing very high data rates over the rich-scattering wireless channel," in *Proc. URSI Int. Symp. Signals, Syst., Electron.*, Pisa, Italy, Oct. 1998, pp. 295–300.
[8] M. M. Ibrahim and A. M. Ibrahim, "Performance analysis of optical receivers with space diversity reception," *IEE Proc. Commun.*, vol. 143, no. 6, p. 369, Dec. 1996.
[9] M. A. Kashani, M. Uysal, and M. Kavehrad, "A novel statistical channel model for turbulence-induced fading in free-space optical systems," *J. Lightw. Technol.*, vol. 33, no. 11, pp. 2303–2312, Jun. 1, 2015.
[10] N. Perlot et al., "18km bidirectional free-space optical link with multi-aperture antenna and DWDM SFP+ transceivers (VERTIGO project)," *Proc. SPIE*, vol. 12413, Mar. 2023, Art. no. 124130W.
[11] U. J. Daly, F. Iga, A. Boldin, A. J. Vallance, M. A. Cox, and M. P. J. Lavery, "Low-complexity turbulence resilience enabled by a multi-mode bi-directional transceiver," *Opt. Exp.*, vol. 32, no. 20, p. 34314, Sep. 2024.
[12] L. C. Andrews and R. L. Phillips, *Laser Beam Propagation Through Random Media*, 2nd ed., Bellingham, WA, USA: SPIE Press, 2005.
[13] L. C. Andrews, *Field Guide to Atmospheric Optics*. Bellingham, WA, USA: SPIE Press, 2019.
[14] *IEEE Standard for Ethernet*, Standard 802.3-2022, Jul. 2022.
[15] W. Eddy, *Transmission Control Protocol (TCP)*, document RFC 9293, RFC Editor, Jul. 2022.
[16] K. Cao, H. Du, J. Zhang, G. Hao, Q. Ran, and J. Ma, "Calculation of average acquisition probability for spiral–circular composite scanning in free space optical communication," *Opt. Commun.*, vol. 532, Apr. 2023, Art. no. 129267.

Authorized licensed use limited to: University of Witwatersrand. Downloaded on October 24,2025 at 06:26:12 UTC from IEEE Xplore. Restrictions apply.